ELSEVIER

Biochimica et Biophysica Acta 1460 (2000) 60–74

BIOCHIMICA ET BIOPHYSICA ACTA
BBA

www.elsevier.com/locate/bba

Review

Chromophore reorientation during the photocycle of bacteriorhodopsin: experimental methods and functional significance

Maarten P. Heyn *, Berthold Borucki, Harald Otto

Biophysics Group, Department of Physics, Freie Universität Berlin, Arnimallee 14, D-14195 Berlin, Germany

Abstract

Light-induced isomerization leads to orientational changes of the retinylidene chromophore of bacteriorhodopsin in its binding pocket. The chromophore reorientation has been characterized by the following methods: polarized absorption spectroscopy in the visible, UV and IR; polarized resonance Raman scattering; solid-state deuterium nuclear magnetic resonance; neutron and X-ray diffraction. Most of these experiments were performed at low temperatures with bacteriorhodopsin trapped in one or a mixture of intermediates. Time-resolved measurements at room temperature with bacteriorhodopsin in aqueous suspension can currently only be carried out with transient polarized absorption spectroscopy in the visible. The results obtained to date for the initial state and the K, L and M intermediates are presented and discussed. The most extensive data are available for the M intermediate, which plays an essential role in the function of bacteriorhodopsin. For this intermediate the various methods lead to a consistent picture: the curved all-*trans* polyene chain in the initial state straightens out in the M intermediate (13-*cis*) and the chain segment between C_5 and C_{13} tilts upwards in the direction of the cytoplasmic surface. The kink at C_{13} allows the positions of β-ionone ring and Schiff base nitrogen to remain approximately fixed.

Keywords: ^{2}H NMR; Linear dichroism; Neutron diffraction; X-ray diffraction; Fourier transform infrared spectroscopy; Bacteriorhodopsin; Purple membrane; Retinal

1. Introduction

Light-induced isomerization of the chromophore plays a major role in the mechanism of the retinal proteins bR, hR and sR and the photoreceptors rhodopsin, phytochrome and photoactive yellow protein (PYP) [1,66]. Rapid isomerization about a unique double bond leads to a changed configuration and orientation of the chromophore in its binding pocket. In subsequent slower thermal steps the altered chromophore structure drives the protein into the activated state. The initially localized structural switch in the chromophore leads ultimately on a slower time scale to structural changes in protein domains which are far away from the chromophore binding pocket (e.g., the altered loops of rhodopsin in M_{II} or the signal transduction domain in phytochrome). How is the changed chromophore structure transmitted to the protein? What is the mechanism of this chromophore–protein coupling? Active reorientational motions of the chromophore play probably an important role in these processes. Even modest movement of the protonated Schiff base in the retinal proteins will lead to significant changes in electrostatic interactions and p*K* values. In a tight binding pocket chromophore reorientation will also lead to direct steric coupling between chromophore methyl groups and side chains of amino acids in the binding

* Corresponding author. Fax: +49-30-8385-6299; E-mail: heyn@physik.fu-berlin.de

0005-2728/00/$ – see front matter
PII: S0005-2728(00)00130-4

pocket. The most dramatic structural evidence for transient chromophore reorientations was obtained for the photoreceptor PYP in which the chromophore changes its orientation transiently by approximately 60° [2].

In the first part of this review we briefly present and discuss the major methods that have been used so far to characterize orientational changes of the chromophore in bR. The purpose of this is to point out the strengths, weaknesses, limitations and pitfalls of these various methods. This should allow the reader to reach her or his own conclusions regarding the reliability and significance of the different experiments. In the second half we will discuss and compare the results obtained for bacteriorhodopsin and its transient intermediates in an integrated way, with emphasis on the M intermediate. For general information and background on bR we refer to the latest previous comprehensive review [1] and to the other articles in this issue.

2. Biophysical methods to characterize chromophore orientation

2.1. Steady-state and transient linear dichroism in the visible, UV and IR

The goal of these experiments is to determine the direction of the chromophore transition dipole moment with respect to the membrane normal in bR and the various intermediates (with oriented samples) or the change in transition dipole direction between bR and the intermediates (with isotropic samples). Fig. 1a shows the planar all-*trans*, 15-*anti* chromophore with protonated Schiff base that occurs in the light-adapted bR state and explains the numbering of the carbon atoms. In dark-adapted state the chromophore of bR exists in a 1:2 equilibrium between the all-*trans*, 15-*anti* and the 13-*cis*, 15-*syn* isomers. The isomeric configuration in bR and in all the intermediates is known mainly from resonance Raman and nuclear magnetic resonance (NMR) experiments. For further details see reviews in [1] and in this issue. In the M intermediate the configuration is 13-*cis*, 15-*anti* and the Schiff bas is deprotonated as depicted in Fig. 1b.

For steady-state measurements oriented samples

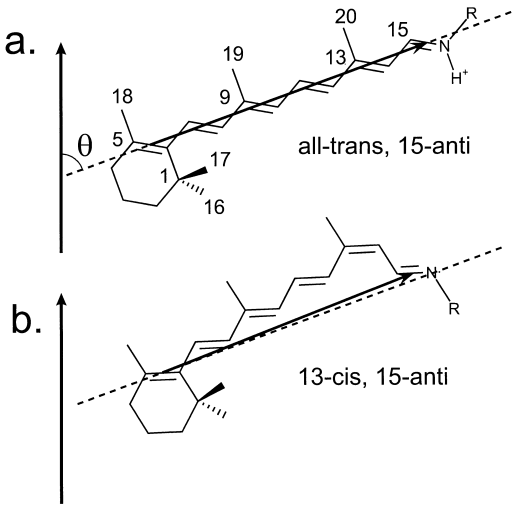

Fig. 1. (a) Numbering of carbon atoms of the all-*trans*, 15-*anti* chromophore with protonated Schiff base. The vector represents the transition dipole moment of the 568 nm band. It is drawn parallel to the C_5–C_{15} direction (- - -) and makes an angle θ of 69.0° with the membrane normal (vertical). (b) Deprotonated Schiff base in 13-*cis*, 15-*anti* configuration as in the M intermediate. With respect to its original direction in a (- - -) the C_5–C_{13} part of the polyene chain is tilted up by 11°. As a consequence the transition dipole moment (arrow) tilts out of the membrane by only about 2°. This reorientation of the C_{19} and C_{20} methyl groups and upward kinking of the chain with C_5 and N staying approximately fixed has been observed in the M intermediate by neutron diffraction, X-ray diffraction, ^{2}H NMR and linear dichroism.

are clearly required. With uniaxially oriented samples the linear dichroism is described by the anisotropy $\bar{r}$

$$\bar{r} = \frac{A_{\parallel} - A_{\perp}}{A_{\parallel} + 2A_{\perp}} = \frac{1}{2}(3\cos^2\theta - 1)\cdot S_2 \qquad (1)$$

where $A_{\parallel}$ and $A_{\perp}$ are the absorptions with light polarized parallel and perpendicular, respectively, to the orientation axis, θ is the angle between the transition dipole moment and the membrane normal and S_2 is the order parameter describing the orientational distribution of the membranes with respect to the orientation axis. Purple membranes can be oriented by drying a suspension under defined humidity on a flat support [3,4] or by centrifugation [5]. In this way membrane films with order parameters close to one can be realized. Alternatively purple membranes may be oriented by modest electric [6,7] or large magnetic fields [8] in suspension. Excellent orientation may also be achieved in a crystal [9]. After embedding purple membranes in an isotropic gel, good orienta-

tion may be achieved by mechanical squeezing or by anisotropic swelling of a dehydrated gel [10]. Purple membranes may also be oriented in a high magnetic field (14T) and subsequently immobilized in a gel [11–13]. In contrast to the partially dehydrated films such gels allow well-defined conditions of pH and ionic strength in an aqueous medium and permit a normal photocycle.

To interpret the orientation of the transition dipole moment in terms of the orientation of the chromophore, it is necessary to know how the transition dipole vector is fixed in the molecular frame. To first order one expects the optical transition dipole moment for the S_0–S_1 transition to be parallel to the polyene chain for all-*trans* retinal, and this is borne out by linear dichroism measurements on retinal crystals [14]. These experiments provided also information about the 11-*cis* and 13-*cis* isomers and suggested that the transition dipole vector approximately connects the C_5 atom of the β-ionone ring with the terminal oxygen atom [14]. The view that the transition dipole moment $\vec{\mu}$ is the vector sum of bond contributions is supported by linear dichroism experiments on bR regenerated with 3,4-dehydroretinal [4]. The extra double bond in the β-ionone ring turns the transition dipole direction by just the amount expected [4]. There is also evidence, however, that the transition dipole for the lowest transition of a simple straight chain polyene may deviate by as much as 20° from the chain direction [15]. Further corrections may be expected in going from a retinal to a retinal model compound with a protonated Schiff base linkage and finally to the chromophore in the bR binding pocket with its interaction with the complex counter ion. Recent quantum chemical calculations suggest that in bR the transition dipole moment makes an angle of 10.5° with respect to the long axis of the polyene chain [16].

Transient linear dichroism measurements provide information on the change in the transition dipole orientation in the various photocycle intermediates. Initially most of these experiments were performed by photoselection with linearly polarized flash excitation of isotropic purple membrane samples [17–19]. Such experiments provide information on Ω_{oi}, the angle between the transition dipole moment in the initial state o and the intermediate state i. In the absence of rotational diffusion the anisotropy of the i^{th} intermediate r_i is given by $r_i = 0.4P_2(\cos\Omega_{oi})$. Since the angular changes Ω_{oi} are expected to be small, such measurements are very insensitive. Ω_{oi} has to be larger than 7° to lead to a barely detectable change in anisotropy of 0.01 (from 0.40 to 0.39, 2.5%). In suspensions the anisotropy decays due to the rotational diffusion of the membranes (on the millisecond time scale). This complicates the analysis of the slow intermediates since the anisotropy has to be extrapolated back in time. By immobilization of the membranes in an isotropic gel the depolarization due to this rotational diffusion may be suppressed. More structural information is obtainable in photoselection experiments with oriented purple membranes, since both the angle between the transition dipole moment and the membrane normal (θ_i) as well as the change in azimuthal angle may be determined [11,20,21]. By exciting with light which is linearly polarized either parallel or perpendicular to the orientation axis, two anisotropies r^V and r^H may be measured, which depend on these two angles in different ways [11,20,21]. Moreover, such measurements with oriented samples are much more sensitive than photoselection experiments with isotropic samples. For the case of perfect orientation and if only one intermediate contributes at the measuring wavelength, we have for example $r_i^V = P_2(\cos\theta_i)$. With θ_i around 69°, the same 7° change in θ_i to 62° discussed above will now lead to a change in r_i^V from −0.307 to −0.169, i.e., a change of 45%. The reason for this dramatic increase in sensitivity is of course that with the oriented samples one measures the angles with respect to the membrane normal. Since this angle is around 69° in the initial state, one is at a much steeper section of the $P_2(\cos\theta)$ curve than with the isotropic samples where the angular change is close to zero and one is in the least sensitive part of the P_2 curve. All photoselection experiments suffer, however, from an intrinsically low signal-to-noise ratio. To avoid errors due to saturation effects only an infinitesimal fraction of the chromophores may be excited in photoselection experiments [11,22]. With a permanently oriented system there is actually no need for photoselection to create an oriented distribution of transition dipole moments. It was recently realized that isotropic excitation of oriented immobilized purple membranes gets completely around these saturation and signal-to-noise problems [12,13,23]. In

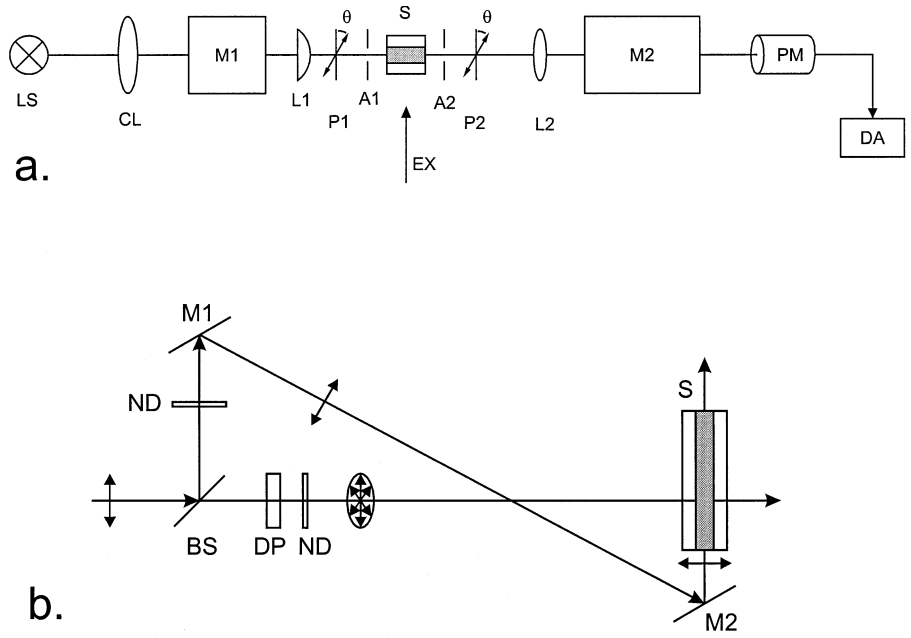

Fig. 2. (a) Experimental setup of the linear dichroism measuring beam [13]. LS, light source; CL, condenser lens; M1, M2, monochromators; L1, L2, lenses; P1, P2, polarizers; A1, A2, apertures; S, sample; EX, excitation; PM, photomultiplier; DA, data acquisition. The orientation axis is perpendicular to the plane of the drawing. At $\theta = 0°$ the polarizers are parallel to the orientation axis. (b) Geometry for isotropic excitation [13]. BS, beam splitter; M1, M2, mirrors; DP, depolarizer; ND, neutral density filters; S, magnetically oriented gel sample in 4×10 mm cuvette. Orientation axis parallel to long side of cuvette.

this case it is permissible and of advantage to excite with high intensities leading to excellent signal-to-noise ratios [12,13]. Errors due to saturation are absent. With isotropic excitation the information about the change in azimuthal angle is lost and r_i is simply given by $r_i = P_2(\cos\theta_i)\cdot S_2$. By placing the oriented sample between parallel polarizers and measuring the transient absorption as a function of the angle between the parallel polarizers and the direction of uniaxial orientation, a further gain in accuracy and information could be achieved [13,23]. In this way also the transient linear birefringence is measured. By using the Kramers–Kronig transform, this information provides an important control on the reliability of the transient linear dichroism data [13,23]. Fig. 2 shows how transient linear dichroism experiments with isotropic excitation of oriented purple membranes are currently performed [13].

The transient linear dichroism is defined analogously to Eq. 1 in terms of the transient absorption differences $\Delta A(\lambda, t)$. With m intermediates with extinction coefficients $\varepsilon_i(\lambda)$, anisotropies r_i and molar concentrations $n_i(t)$, we then have for the observed anisotropy $R(\lambda,t)$ the following expression:

$$R(\lambda,t) = \frac{\Delta A_{\parallel}(\lambda,t) - \Delta A_{\perp}(\lambda,t)}{\Delta A_{\parallel}(\lambda,t) + 2\Delta A_{\perp}(\lambda,t)} = \frac{\sum_{i=1}^{m} n_i(t)[\varepsilon_i(\lambda) r_i - \varepsilon_0(\lambda) r_0]}{\sum_{i=1}^{m} n_i(t)[\varepsilon_i(\lambda) - \varepsilon_0(\lambda)]} \quad (2)$$

ε_0 and r_0 are the extinction coefficient and anisotropy, respectively, for the initial state bR. Eq. 2 illustrates the problems in analyzing the observed $R(\lambda,t)$. First, singularities will occur whenever the denominator in the ratio of R becomes zero. Second, how to extract the anisotropy r_i of a single intermediate, when it is well known that in general the spectra of most intermediates overlap strongly and that they usually coexist. If at a particular time only one intermediate i exists, Eq. 2 reduces to

$$R(\lambda,t) = \frac{\varepsilon_i(\lambda) r_i - \varepsilon_0(\lambda) r_0}{\varepsilon_i(\lambda) - \varepsilon_0(\lambda)} \quad (3)$$

If, moreover, regions of wavelength exist where only intermediate i absorbs, Eq. 3 reduces to $R(\lambda,t) = r_i$.

Such an approach works in exceptional cases such as the O-intermediate at 690 nm at times beyond 3 ms [12]. Another useful approach to analyze Eq. 2 uses the amplitude spectra [12]. Recently a new formalism was developed which extracts the anisotropies r_i, the spectra $\varepsilon_i(\lambda)$ and the time courses $n_i(t)$ of the photocycle intermediates in a model-independent way from the combined analysis of the transient absorbance and linear dichroism data [13,23]. This analysis is based on only two plausible assumptions: (1) the sum of the intermediate concentrations is constant in time in the early part of the photocycle (up to M), (2) the M intermediate does not absorb beyond 520 nm.

Absorption measurements with linearly polarized light with oriented purple membranes have also been carried out in the infrared region [24–28]. These steady-state Fourier transform infrared (FTIR) measurements were performed with oriented multilamellar films. The K, L or M intermediates were accumulated by illumination at appropriate low temperatures. In order to reduce the contribution of water, the samples were usually fairly dehydrated. Dichroic data are commonly collected by performing a series of measurements at various tilt angles between the plane of the oriented films and the beam direction. No time-resolved measurements have been reported.

The FTIR data are collected as difference spectra between the trapped intermediate and the initial bR state. Of main interest in the linear dichroism studies are the strong bands due to the C=C stretching modes in the various intermediates (varying between 1514 cm^{-1} in K and 1564 cm^{-1} in M), the strong C–C stretching modes between 1160 and 1260 cm^{-1} and the hydrogen out-of-plane (HOOP) modes between 930 and 980 cm^{-1}. As for the linear dichroism in the visible, the interpretation of these dichroism experiments depends on knowledge of the location of the transition dipole moments in the molecular frame. For the HOOP modes $\vec{\mu}$ is expected to be approximately perpendicular to the polyene plane [24]. The dichroism of the HOOP modes may thus be used to obtain information on the orientation of the polyene plane with respect to the plane of the membrane. The oscillator strength of the ethylene stretching modes is mainly due to the central $C_{11}=C_{12}$ bond with smaller contributions from the $C_9=C_{10}$ and $C_{13}=C_{14}$ bonds [24]. Normal coordinate calculations show that the most intense C=C modes involve in-phase mixings of a number of C=C bonds. It has been argued that the transition dipole moment in that case is roughly parallel to the polyene chain axis and not to the C=C bond direction [24]. No polarized FTIR measurements have been carried out with retinal model compounds to verify this point. The dichroism in the C=C and C–C modes may thus be used to investigate the orientation of the polyene chain or of individual carbon–carbon bonds.

2.2. *Solid-state deuterium NMR with oriented purple membranes regenerated with retinal selectively deuterated in the methyl groups*

This method utilizes the well-known orientational dependence of the deuterium quadrupole splitting $\Delta\nu_Q$ on the angle between the deuterium quadrupole tensor and the magnetic field [29]. For the case of the deuterated methyl groups of the chromophore of bacteriorhodopsin the fast motional limit applies [30] and the quadrupole splitting is given by

$$\Delta\nu_Q = \Delta\nu_Q^{powder}(3\cos^2\theta - 1) \quad (4)$$

with $\Delta\nu_Q^{powder}$ approximately 40 kHz. The angle θ is the angle which the axis of the deuterated methyl rotor C–C^2H_3 makes with the magnetic field. For the special case of perfect orientation with all purple membranes in the sample perpendicular to the magnetic field and neglecting membrane curvature, each methyl rotor makes the same angle θ with the field and the angle can be calculated directly from the quadrupolar splitting using Eq. 4. The goal of these NMR experiments is to determine the angle between the methyl bond direction and the membrane normal. In the geometry described (zero tilt) the membrane normal is parallel to the magnetic field and the bond angle equals θ. It is apparent from Eq. 4 that we cannot distinguish between θ and its supplement $\pi-\theta$. Moreover, when $|\Delta\nu_Q| \leq |\Delta\nu_Q^{powder}|$, i.e., when $35.3° \leq \theta \leq 90°$, there are two solutions to Eq. 4. This ambiguity can be readily resolved by measuring the quadrupolar splitting at various tilt angles between the oriented membrane sample and the magnetic field [31–34]. To use Eq. 4 we clearly need an oriented sample. The analysis so far assumed that the orien-

tation was perfect and that the membranes are flat. The bR samples used in these experiments consisted of hydrated multilayers of purple membranes. Such oriented layers are produced by drying a suspension of purple membranes at defined humidity on a glass support. It is well-known that these oriented films exhibit considerable mosaic spread (order parameter $S_2 < 1$). As the film gets thicker the orientational disorder builds up. Thus rather than having a single angle θ in Eq. 4 at zero tilt, we have a distribution of angles leading to line broadening. Therefore a proper line shape simulation is essential in the analysis of these NMR experiments. It was recently shown that it is necessary to take the three-dimensional (3D) character of the mosaic spread properly into account [34,35]. A highly efficient Monte Carlo procedure has been introduced, which allows arbitrary angular distributions to be used in the line shape simulation [34]. In many cases a Gaussian probability distribution for the angle α between the local membrane normal and the macroscopic uniaxial sample normal

$$e^{-\alpha^2/2\sigma^2} \tag{5}$$

is adequate to describe the mosaic spread. In Eq. 5 we define σ as the mosaic spread. For well-ordered purple membrane samples σ is of the order of 7–10° [34]. The mosaic spread is usually a parameter in the line shape simulation. Its value is not arbitrary however, since independent measurements such as lamellar X-ray or neutron diffraction [36] and the ^{31}P chemical shift anisotropy of the lipid headgroups constrain its value. With similarly prepared samples the mosaic spread measured by lamellar neutron diffraction [36] was only slightly smaller.

The quality and success of the line-shape simulation is determined from an analysis of the residuals. Five parameters enter the simulation, viz., the coupling constant $\Delta\nu_Q^{powder}$, the intrinsic line width, the mosaic spread σ, the sample tilt and the bond orientation. The latter is the structural information of interest. The first two parameters were determined from a powder-sample and a T_2 relaxation experiment, respectively [34], and can therefore vary only in a very narrow interval. Likewise the sample tilt can only deviate a few degrees from the set angle. This leaves as the remaining parameters the mosaic spread and the bond orientation. Usually data are collected at a number of tilt angles in the initial bR and M states with the same sample. All of these data are simulated simultaneously. The common parameters from all of these experiments ($\Delta\nu_Q$, line width, σ) are therefore even better defined. Moreover, the bond orientation is independent of the tilt angle, and consequently, the entire tilt series in one state of the sample must be fitted with the same value for this parameter, again increasing its precision. As a result, the uncertainty in the determination of the bond angle from all spectra taken together is not larger than 3°. Fig. 3 shows the results from a tilt series with a sample deuterated in the C_1–$C_{16}^2H_3$ bond together with the line shape simulations [34]. The excellent agreement between data and simulation over the entire range of tilt angles from 0° to 90° is apparent from the residuals.

Whereas solid-state deuterium NMR is a very accurate structural method to determine bond orientations, it is an insensitive method in terms of amounts of sample. Typically these experiments require 80 mg of bacteriorhodopsin that is specifically deuterated in one methyl group ($^2H_3$). The first step in the sample preparation is the synthesis of the specifically deuterated retinal. The deuterated retinal can be incorporated in purple membranes by adding it to the growth medium of a retinal deficient mutant or by regeneration of a bleached apomembrane [37,39]. Oriented films are usually prepared by drying of a concentrated suspension in 86% relative humidity (saturated solution of KCl) on 0.3-mm thick glass plates. Using spacers the plates are assembled pairwise into sandwiches with the membrane films facing each other. Approximately 15 of these sandwiches are assembled into a stack inside the round 10-mm diameter NMR tube. It is essential that the films remain fully hydrated. Using samples with the sides of the sandwiches open the NMR tube has to be tightly closed and the plates have to be rehydrated in a closed box after each experiment. As an alternative the sandwiches can be sealed on the edges by using an appropriate glue. Dehydration of the films prevents the formation of the M intermediate. To trap bacteriorhodopsin in the M intermediate, the life time of this intermediate has to be increased sufficiently. This can be achieved at −50°C either by applying 0.5 M guanidine hydrochloride at pH 9.5

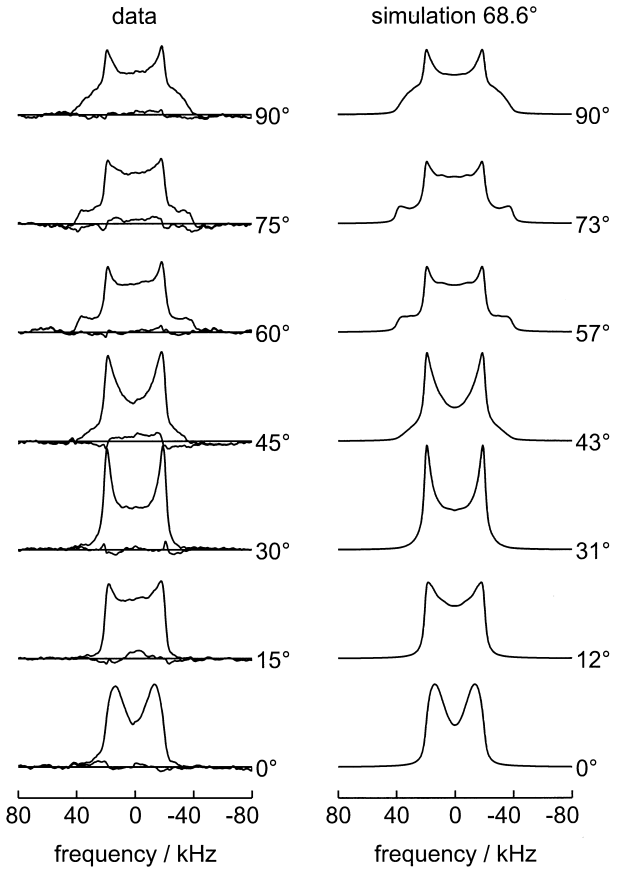

Fig. 3. Experimental ^{2}H NMR tilt series and spectral simulations for C_1–$C^2_{16}H_3$-labeled bR at −50°C [34]. The left panel shows the data (250 000 acquisitions for each tilt angle) and their deviation from the fit. The right panel shows that an excellent global fit was achieved with one set of parameters (bond angle 68.6°, mosaic spread 8.7°) for each tilt angle. The angles next to the spectra refer to the tilt angle set in the data collection and the angle used in the simulation, respectively. A deviation of 3° from the set tilt angle was allowed in the simulation.

[40–42] or by using a mutant such as D96A [42]. For experiments on the M intermediate each plate is individually bleached at +5°C and each bleached sandwich is sequentially transferred to the precooled NMR tube which is kept on dry ice. For experiments on M it is essential that a check is made after the data acquisition that all plates are still bleached [42].

The ^{2}H NMR data are acquired with the standard quadrupolar echo sequence [32,42]. Because of the broad quadrupole spectrum a short 90° pulse length of 3–4 μs is desirable [34]. Typically up to 3 million echoes are acquired for a single tilt angle [42]. With a recycle time of 200 ms, these experiments are very time consuming and require very high stability of the NMR spectrometer. Under optimal conditions a signal-to-noise ratio of up to 100 can be achieved [34,42].

Recently an interesting modification of this solid-state NMR approach was described [43,44]. In these experiments, the stack of oriented purple membranes is packed in a magic angle spinning rotor in such a way that the average membrane normal is parallel with the rotor axis. The static deuterium NMR spectrum described above is then sampled at the spinning side band frequencies. One potential advantage of this method is that the intensity is only sampled at the discrete and narrow side-band frequencies thus allowing higher sensitivity. Another advantage is that the line broadening caused by the mosaic spread collapses at the magic angle, thereby leading to improved spectral resolution. In the first application of this method to the deuterated chromophore of bR, however, at a rotor frequency of 4040 Hz no significant improvements were yet apparent [43].

2.3. *Neutron diffraction with oriented purple membrane multilayers*

Neutron diffraction with purple membranes that are regenerated with specifically deuterated retinals was instrumental in determining the position of the chromophore inside bacteriorhodopsin before such information became available from cryo electron microscopy [37–39]. In these experiments the scattering intensity differences are measured between samples with specifically deuterated chromophores and with perprotonated chromophores. One advantage of neutron scattering is that the change in scattering strength caused by the replacement of ^{1}H by ^{2}H is substantial. Another major advantage is that the labeling is isomorphic since this isotopic replacement leaves the chemistry unchanged. All of these experiments were performed with multilamellar oriented films. The natural two-dimensional P_3 lattice was used to determine the chromophore label density in the plane of the membrane [37–39]. Lamellar diffraction was employed to find the label positions in the direction perpendicular to the membrane [36]. Initially these experiments were performed at room temperature with purple membrane films at 86% relative humidity that were oriented on quartz slides. Typi-

cally the mosaic spread of these films was $< 10°$ full-width at half-maximum. Three samples with different label distributions were used: six deuterons in the C_{19} and C_{20} methyl groups [37], five deuterons in the C_{20} methyl group and on C_{14} and C_{15} [39], eleven deuterons in the β-ionone ring [38]. The centers of deuteration of these three labels were the middle of the chain (C_{11}), the Schiff base end of the chain (near the C_{20} methyl group) and the β-ionone end of the chain (near C_1). Since the data collection at room temperature took several days and the hydrated membranes were kept in a closed aluminum can, these data were for the dark-adapted state. Experiments in M were performed at 90 K with samples that were soaked in 0.1 or 1 M guanidine hydrochloride at pH 9.6 [40]. Great care was taken to bring bR completely into the M state by illumination at +5°C followed by rapid cooling to 90 K in the absence of light. The reference label positions in bR were determined at the same temperature of 90 K. Again the sample was illuminated at +5°C, but after turning off the light and before cooling to 90 K the sample was allowed to return to the light-adapted ground state. In this way the label positions were determined for the light-adapted state. The phase information and the intensity ratios of overlapping reflections that are required in the data analysis were obtained from electron microscopy.

2.4. X-Ray diffraction with 3D-crystals

The X-ray diffraction work with 3D-crystals of bacteriorhodopsin is described in detail in another article in this issue, as well as in [45–50].

3. Chromophore orientation in bR and the photocycle intermediates K, L and M

3.1. Initial dark-state bR

The most extensive information about the chromophore orientation is available for bacteriorhodopsin in the initial state. All the methods described in the previous section have been applied to this state. Low-resolution data are available from neutron diffraction and linear dichroism. The more detailed structural information of higher resolution comes from X-ray diffraction and deuterium NMR. The results obtained for the polyene chain orientation and the orientation of the C–CH_3 bonds are collected in Tables 1 and 2.

A large number of experiments have been performed to determine the orientation of the electronic transition dipole moment with respect to the membrane normal. Linear dichroism experiments with oriented purple membrane films lead to values of 71° [3], 70.3° [4], 70° [51] and 69° [5]. Linear dichroism measurements with magnetically oriented purple membranes that are immobilized in optically clear aqueous gels result in angles of 66.8° [11] and 66.6° [21]. With electrically oriented purple membranes in aqueous suspension values of 69.5° [6] and 69° [7] were obtained. In crystals where no mosaic spread corrections are required, the value was 68.5° [9]. These values from nine independent measurements exhibit only a small spread around the average value of 69.0°. In some of these experiments an attempt was made to detect orientational differences between the light-adapted all-*trans* form and the 13-*cis*, 15-*syn* isomer that contributes 67% to the dark-adapted form. No difference in anisotropy between the light- and dark-adapted states was observed in [10,23], whereas a very small angular change of 0.4° was detected in [9] and [6].

Polarized FTIR difference spectra have been measured for the K, L and M intermediates [24–28]. The depletion signal in each of these experiments provides information on the orientation of the transition dipole moment for the C=C and C–C stretching modes in the initial bR state. Although these angles should be the same, the values from the K difference spectra (at 81 K) [24] were consistently larger than the values from the M difference spectra (performed at 250 K). For the C=C stretch in bR the value was 73° from the bR-K and 69° from the bR-M difference spectrum [24]. For the various C–C stretch modes the differences were even larger: C_8–C_9: 84° (K), 66° (M); C_{10}–C_{11}: 85° (K), 64° (M); C_{12}–C_{13}: 84° (K), 71° (M); C_{14}–C_{15}: 80° (K), 70° (M). The authors concluded that the orientation is temperature dependent with the angle increasing with decreasing temperature. Such large angular differences at these two temperatures would preclude a comparison with the results from linear dichroism and neutron diffraction experiments at room temperature. Deuterium

NMR experiments suggest, however, that the orientation is temperature independent, since the orientation of the C_1–C_{16} bond was unchanged between −60° and +20°C [34]. The values from the M experiment (250 K), 69° for C=C and an average value of 67.8° for the four C–C modes are on the other hand in quite good agreement with the average value of 69.0° for the electronic transition dipole moment. From this overall agreement it appears likely that both the electronic and infrared transition dipole moments are to a good approximation parallel to the polyene chain direction in the all-*trans* isomer. Using a photoselection method the angles between the optical and IR transition dipoles (C=C and C–C) projected on the membrane plane were measured directly [27]. It was concluded that this angle is essentially zero and that the transition dipoles are parallel. For the C=C stretch mode in bR at 20°C these authors obtained 66±4° from bR-M difference spectra [28]. From bR-L difference spectra (obtained at 160 K) a value of 74° was obtained for the C=C transition dipole angle in bR [25].

Linear polarization FTIR experiments provided important early information on the average orientation of the plane of the chromophore. From the polarization of the HOOP mode bands it was established that this plane is to a good approximation perpendicular to the plane of the membrane in bR (90±20° [25], 80° [24]).

In-plane neutron diffraction experiments provided the positions of two deuterated labels at the Schiff base and β-ionone ends of the chromophore in the light-adapted state [40]. The centers of deuteration of these two labels with 5 and 11 deuterons are at well defined positions in the molecular frame of the all-*trans* chromophore. The vector connecting these two centers of deuteration makes an angle of 15° with the polyene chain. Using the information that the average plane of the chromophore is perpendicular to the membrane, the angle between the polyene chain and the membrane normal can then be calculated from the in-plane distance between the label positions. In this way an angle of 66° was obtained [40], which in contrast to linear dichroism measurements is independent of knowledge of the orientation of the transition dipole moment in the molecular frame. These data were collected at 90 K.

The high-resolution X-ray diffraction data allow the most accurate determination of the angle between the polyene chain and the membrane normal. When we define the polyene chain direction as the direction of the vector connecting C_5 and C_{15}, the value of 68.7° is obtained for the light-adapted D96N mutant at 1.8 Å resolution [48], in very good agreement with the results from the other methods.

From the ^2H NMR spectra the angles between the C–C^2H_3 bond directions and the membrane normal were calculated [32,34,42,43]. Assuming an untwisted

Table 1
Orientation of chromophore polyene chain with respect to membrane normal in bacteriorhodopsin and in the M intermediate

bR				M		
Method		Angle	Ref.	Angle	$\Delta\theta$	Ref.
1 Optical transition dipole						
Steady-state		69.0°[a]	[][a]	66.9° [9]	−1.8°[c]	[9,23]
Transient					−1.9°[d]	[11,13]
2 Neutron diffraction with 2D-crystals		66°	[40]	55°	−11°	[40]
3 X-Ray diffraction with 3D-crystals						
C_5–C_{15}		68.7°	[48]	68.0°	−0.7°	[48]
C_5–C_{13}		64.8°	[48]	56.6°	−8.2°	[48]
4 Infrared transition dipole						
C=C	bR-M (293 K)	66°±4°	[28]			
C=C	bR-M (250 K)	69°	[24]	62°	−7°	[24]
C–C	bR-M (250 K)	67.8°[b]	[24]			

[a]Average of nine experiments [3–7,9,11,21,51].
[b]Average of four C–C modes.
[c]Average of [9] and [23].
[d]Average of [11] and [13].

planar chromophore structure perpendicular to the membrane plane, the values of 37°, 40° and 32° obtained for the C_5–C_{18}, C_9–C_{19} and C_{13}–C_{20} bonds may be translated into an *average* angle between the polyene chain and the membrane normal of 54°. There is no reason, however, to interpret the difference with the previous values around 68°, 69° as a discrepancy. Small out-of-plane twists on the order of 10–15° were observed [25] and will reestablish the agreement. It is not possible to calculate the polyene chain direction from the NMR results without additional structural information.

The results about the polyene chain direction in bR are summarized in Table 1 and show remarkable consistency and agreement. The FTIR results seem to indicate a temperature dependent orientation for which there is no evidence from the other methods. The scattering in the IR results is more likely due to experimental inaccuracy.

The orientations of the methyl groups were determined by X-ray diffraction [45–50], cryoelectron microscopy [52] and ^{2}H NMR [32,34,42,43]. The results for bR and M are collected in Table 2. In this table only the X-ray diffraction results for the mutant D96N [48] are cited, since this is the only system for which the results are available both in the light-adapted bR state and M intermediate. Both the ^{2}H NMR and X-ray data show that in bR the polyene chain is not straight, but curved in a way that is similar to that observed in the high-resolution crystal structure of the all-*trans* Schiff base model compound *N*-methyl-*N*-phenylretinal iminium perchlorate [53]. Whether a true discrepancy exists depends on the estimated errors. For the ^{2}H NMR experiment the errors are estimated to be ± 3° (see Section 2.2). The X-ray papers do not contain estimates of the errors in the chromophore angles. However, one may get a rough feeling for these errors by looking at the variability of the bond angles for the various structures deposited in the protein data bank, not all of which have yet been published. For this comparison to be meaningful we should limit ourselves to structures of similar resolution. We therefore only consider the structures with PDB file names 1C8R ([48], 1.8 Å resolution), 1C3W ([47], 1.55 Å resolution), 1CWQ (2.25 Å resolution) and 1QHJ ([49], 1.90 Å resolution), all of the same space group. Calculating the angles from these structures, the C_5–C_{18} bond angle varies from 33.4° to 39.8° with an average value of 36.1°. For the C_9–C_{19} bond the values vary between 33.8 of 41.3°, with an average of 37.1°. For the C_{13}–C_{20} bond the range is from 19.0 to 23.2° with an average of 21.6°. It therefore seems that an angular error of ± 3° is also realistic for the X-ray results. In view of these errors it appears therefore from Table 2 that the agreement between the two methods is excellent for the C_5–C_{18} bond and good for the C_9–C_{19} bond. For the C_{13}–C_{20} bond there is a difference of about 10° for all the structures, so that for this bond a true discrepancy seems to exist. Concerning the possible source of this difference, we point out that there are several differences between the two methods. In diffraction the *R* factor is minimized globally over the whole structure subject to the local stereochemical constraints. ^{2}H NMR is a local structural method and only one bond angle is determined directly. Moreover, in NMR each bond angle is determined in a separate independent experiment,

Table 2
Orientation of chromophore C–CH_3 bonds with respect to membrane normal in bR and in the M intermediate

Bond	bR			M		
	X-Ray [48]	^{2}H NMR		X-Ray [48]	^{2}H NMR	Ref.
C_5–C_{18}	33.4°	37°	[32]	35.1°	38.8°	[42]
		36°	[42]		22°	[43]
C_9–C_{19}	34.1°	40°	[32,42]	42.2°	47.5°	[42]
					44°	[41]
C_{13}–C_{20}	23.2°	32°	[32]	37.2°		
C_1–C_{16}	83.9°	68.7°	[34]	77.6°	73°	[42]
C_1–C_{17}	72.9°			64.2°		

whereas in diffraction all angles are obtained from the same experiment.

3.2. K intermediate

Time-resolved linear dichroism measurements on the K intermediate were performed by photoselection in suspension [17,19,54], by photoselection with oriented membranes [21] and by isotropic excitation with oriented membranes [13]. As discussed in Section 2.1, photoselection experiments in suspension are quite insensitive. Overall angular changes of at most 10° [17] and less than 8° [19] were reported with this method. Only one group reported a change as large as 11° [54] with the direction corresponding to an upward tilt of the chain. The much more sensitive measurements with oriented membranes, however, lead to very small changes of 0.8° [13] and 2.9° [21] with the angle with respect to the membrane normal becoming smaller. Recently an X-ray diffraction study at 110 K was reported on the low-temperature K intermediate [50]. This low temperature K_{LT} differs from the room temperature K by a more distorted non-planar geometry. In the X-ray structure of K_{LT} the atoms of the β-ionone ring and the polyene chain up to C_{12} remain fixed, with small local movements of the C_{13}, C_{20}, C_{14}, C_{15} and N atoms at the Schiff base end of the chain where the isomerization occurs. The C_5–C_{15} direction changes only from 69.7° in bR [49] to 70.0° in K_{LT} [50], in excellent agreement with the transient linear dichroism measurements [13]. In steady-state IR linear dichroism experiments at 81 K, the orientations of the C=C transition dipole moments in K (1514 cm^{-1}) and bR (1530 cm^{-1}) were found to be 79° and 73°, respectively [24]. The authors concluded, however, that 'the transition moment of ...K... is parallel to that of bR within the range of error' [24].

3.3. L intermediate

All transient dichroism experiments on L come to the same conclusion that the angle of $\vec{\mu}$ with the normal is smaller than in bR [13,54,55]. The insensitive photoselection experiments with isotropic suspensions or gels resulted in rather large values of 11° [54] to 15° [55] for the change in angle. More recent measurements with the more sensitive method

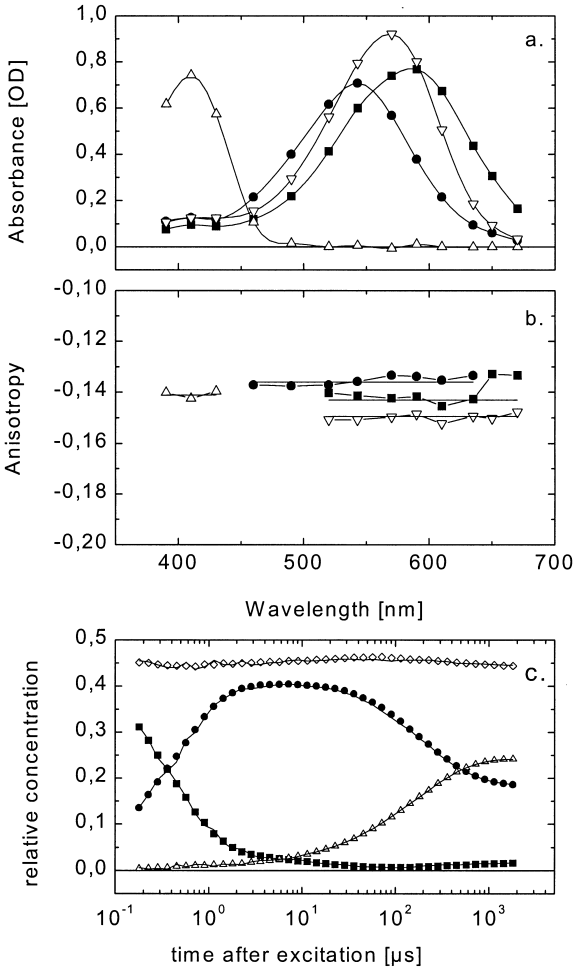

Fig. 4. Results of the combined analysis of transient absorbance and linear dichroism data for the mutant D96A (pH 4.7, 50 mM KCl, 20°C) [13]. ■, K; ●, L; △, M; ▽, bR; ◇ in (c), sum of the relative concentrations of K, L and M. (a) Intermediate spectra; (b) anisotropies; (c) time courses.

using oriented membranes led to much smaller angular changes of −2.7° [21] and −1.7° ± 0.3° [13]. These small values are in line with corresponding small changes in the K and M intermediates. They are to be expected if isomerization only leads to structural changes in the region C_{13} to N (as in K) or if doming occurs (as in M, see below and Fig. 1b). Fig. 4 provides an example of the current quality of the transient dichroism experiments with oriented purple membranes and isotropic excitation [13]. As is apparent from Fig. 4c, in the mutant D96A the decay of K is accelerated, leading to a large accumulation of the L intermediate. This mutant is thus well suited for investigations on L. The combined transient absor-

bance and anisotropy data at 12 wavelengths and 10 polarization angles were fitted globally, leading to unique spectra (Fig. 4a), time courses (Fig. 4c) and anisotropies (Fig. 4b) for the intermediates. Clear differences in the anisotropies of K, L, M and bR exist and these are approximately constant over the absorption band of each intermediate. Fig. 4b shows that the largest difference in anisotropy occurs between bR and L, corresponding to an angular change of $-1.7° \pm 0.3°$ [13].

3.4. M intermediate

This functionally most interesting intermediate can be trapped very easily and has been investigated in greatest detail. Diffraction experiments with two-dimensional purple membrane lattices showed that in this intermediate a major protein conformational change occurs involving helices F and G [56–59].

Using the mutants D96N and D96A, in which the M intermediate has a very long lifetime, the orientation of the optical transition dipole moment could even be measured under steady-state illumination at room temperature [9,23]. With crystals of D96N it was found that the angle is $2.2 \pm 0.5°$ smaller in M [9]. With magnetically oriented purple membranes of D96A at pH 8.0 an angular change of $1.4 \pm 0.3°$ in the same direction was obtained [23]. One advantage of these steady-state experiments over transient experiments is that complete conversion to the M state can be achieved, so that the unknown anisotropy of the higher transitions of bR around 400 nm can be neglected.

The direction of this transition dipole moment change has been confirmed in time-resolved linear dichroism measurements at room temperature. Considerable disagreement exists, however, about the size of the change. In photoselection experiments with magnetically oriented purple membranes a change of 2.7° was detected [11,20]. Using isotropic excitation of magnetically oriented purple membranes a change of only $1.1 \pm 0.3°$ was observed [13]. In these experiments the pH was varied between 4.7 and 7 and no difference in orientation was detected [13]. As explained in Section 2.1, such measurements with oriented membranes are most sensitive to small angle changes. Using photoselection with a pseudo-null method and a suspension of purple membranes no orientational change could be detected implying that the angular change in early M (< 50 μs) is less than 8° [19]. No significant difference between the anisotropy of early and late M was observed in any of these time-resolved measurements. Much larger orientational changes were consistently reported only from one laboratory using the photoselection method with suspensions, which suffers from lack of sensitivity and from saturation errors. These authors measured angular changes as large as −20° in M [54,55]. Moreover, they detected a strong pH dependence of the chromophore orientation, with the largest angular change occurring between pH 6–8 [55]. In order to explain their anisotropy results a so-called 'spectator' model had to be introduced in which non-excited bR molecules reorient during the photocycle of neighboring excited bR molecules [55,60]. There is no evidence for the existence of such rotation from any other method.

What would one expect for the change in orientation of $\vec{\mu}$ if the isomerization occurred near the Schiff base end of the chain, with the polyene chain between C_5 and C_{13} remaining fixed? With reference to Fig. 1a and with the transition dipole vector connecting C_5 and N, we conclude that in that case we would have expected the transition dipole to tilt into the plane of the membrane by about 9°. Instead experimentally it tilts out of the plane by between 1°and 3°. Fig. 1b shows how these observations may be reconciled, if the C_5 to C_{13} part of the chain tilts out of the membrane plane by 10–12°. This argument assumes that the plane of the chromophore remains approximately perpendicular to the plane of the membrane as is indeed the case (see below).

This interpretation of the dichroism data, suggesting a sizable change in the orientation of the polyene chain between C_5 and C_{13}, is supported by neutron diffraction experiments with deuterated chromophores in M [40]. In these experiments it was observed that the in-plane position of the β-ionone ring was unaltered in the transition to M, but that the in-plane position of the labeled C_{13} methyl group moved significantly by 1.4 ± 0.9 Å towards the ring. Translated in angular change this implied that the chain between C_5 and C_{13} tilted out of the membrane plane by $11 \pm 6°$ [40]. Together the linear dichroism and neutron diffraction results suggested that the isomerization leads to movement mainly of the C_{20}

methyl group with the direction C_5–N remaining about the same [20,40]. It was concluded that the C_{20} methyl group moves in M by about 1.7 Å towards the cytoplasmic side of the membrane [20,40].

Recently the structure of bacteriorhodopsin in the M intermediate was solved at a resolution of 2.0 Å using the mutant D96N at 100 K [48]. The M intermediate was produced by illumination at 290 K so that the results for this structure may be compared with those from neutron diffraction [40] and ^{2}H NMR [42] experiments in which the M intermediate was trapped in the same way. The light-adapted structure of the D96N mutant was also solved, at a resolution of 1.8 Å [48]. In good agreement with the optical linear dichroism experiments the orientation of the C_5–C_{15} direction changes only from 68.7° in bR to 68.0° in M [48]. The C_5–C_{13} part of the chain undergoes, however, a much larger reorientation, from 64.8° in bR to 56.6° in M, a change of −8.2° [48]. The X-ray diffraction results are thus in excellent agreement with the neutron diffraction and linear dichroism results. In M the C_{20} methyl group was found to move by 1.3 Å in the direction of the cytoplasmic surface [48], in good agreement with the earlier estimate of 1.7 Å from the low-resolution neutron diffraction and linear dichroism data [20,40].

Solid-state ^{2}H NMR experiments also clearly show that the polyene chain is tilted out of the plane of the membrane in M. The initial experiments with samples of large mosaic spread that were only partially in M and with low signal-to-noise ratio led to a reorientation of the C_9–C_{19} bond of 4° [41]. Recent experiments of much better signal-to-noise ratio, with completely bleached M samples and with a correct line shape simulation show that the orientation of the C_9–C_{19} bond changes by 7.5° in M [42]. The data of Fig. 5 provide clear evidence for spectral and orientational changes between the light-adapted bR state and the M intermediate [42]. The values of the methyl bond orientations determined by X-ray diffraction and ^{2}H NMR are collected in Table 2. As can be seen from this table, this change of +7.5° is in excellent agreement with the change of +8.1° obtained by X-ray diffraction for the same bond [48]. Moreover, these local changes at the C_9–C_{19} bond are in excellent agreement with the change in the C_5–C_{13} part of the polyene chain of 8.2° (X-ray diffraction), 11° (neutron diffraction) and 11° (interpretation of the linear dichroism experiments). The angular change of the C_5–C_{18} bond is smaller. Here the X-ray and ^{2}H NMR experiments show again good agreement: +1.7° from X-ray diffraction [48] and +2.8° from ^{2}H NMR [42]. Application of the new MAS method led, however, to the observation of an apparent change of −14° [43]. The source of this discrepancy remains unclear, but the agreement between fit and simulation was unsatisfactory and possibly a mixture of early and late M intermediates was trapped [43].

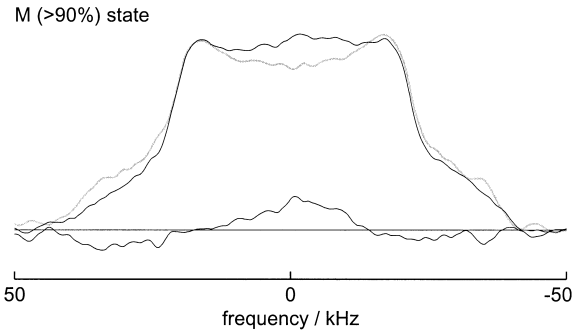

Fig. 5. ^{2}H NMR spectra from wild-type bacteriorhodopsin regenerated with C_9–$C^2_{19}H_3$-labeled retinal and treated with a guanidine hydrochloride solution to trap M [42]. Data were taken at −50°C at zero tilt. The spectra of the light-adapted bR state (gray line) and the M intermediate (black line) are superimposed. Each spectrum consists of 1.6 million acquisitions collected over 4 days. The difference between the two spectra (bottom) shows clearly that intensity shifts toward the carrier frequency (0 kHz) indicating an angle increase in M.

From the linear dichroism in the HOOP modes in M it was concluded that the plane of the chromophore makes an angle of 80° with the plane of the membrane [24]. This conclusion that the two planes are approximately perpendicular is also supported by polarized resonance Raman spectra of the C=C modes [61].

The dichroism of the ethylenic C=C stretching vibration at 1565 cm^{-1} provides information on the polyene chain orientation. In [27,28] it was concluded that the dichroism in M was the same as in bR indicating the same orientation. In [24] the angle for the C=C stretch at 1563 cm^{-1} was 62°, i.e., 7° smaller than these authors found for the C=C stretch of bR (1526 cm^{-1}) at the same temperature. This difference was, however, smaller than the errors and was not considered significant by the authors. In fact they stated that '... overlap with another band near 1554

cm^{-1} precludes an accurate determination of θ_T' [24]. If we nevertheless take these measurements seriously, we have to keep in mind that the in-phase C=C stretch mode is mainly localized on the $C_{11}=C_{12}$ and $C_9=C_{10}$ bonds. The change of 7° degrees is thus in good agreement with the X-ray diffraction, neutron diffraction and optical linear dichroism measurements. There is no contradiction between the optical and vibrational linear dichroism results, since the former measures the orientation of the complete conjugated system (C_5–C_{15}) whereas the latter measures mainly the orientation of the chain near the C_{11}–C_{12} bond (i.e., before the kink at C_{13}).

Taken together, the results of these experiments show a remarkably consistent picture. After isomerization and relaxation to the M intermediate, the C_5–C_{15} direction is barely changed, the β-ionone ring and Schiff base nitrogen move slightly towards each other along the initial C_5–C_{15} direction, the initially strongly curved polyene chain straightens out in M and the C_5–C_{13} portion of the polyene chain tilts towards the cytoplasmic side of the membrane (see Fig. 1b). The movement of the C_{13} methyl group by 1.3 Å leads to a corresponding movement of the indole ring of W182 [48]. This steric interaction between the C_{13} methyl group of the chromophore and the indole ring of W182 in helix F may be an important step in the coupling between chromophore and protein motions. Helix F is one of the helices that show structural changes in M [56–59]. A number of experiments point to an important functional role for this interaction between the C_{13} methyl group and W182 [62–65].

Acknowledgements

We thank Dr H. Luecke and Dr S. Moltke for helpful discussions and critical comments. We thank the National Institutes of Health (Grant GM 53484) and the Deutsche Forschungsgemeinschaft (Sfb 498, B1) for financial support.

References

[1] M. Ottolenghi, M. Sheves, Isr. J. Chem. 35 (1995) 193–515.
[2] U.K. Genick, G.E.O. Borgstahl, K. Ng, Z. Ren, C. Praderwand, P.M. Burke, V. Srajer, T.-Y. Teng, W. Schildkamp, D.E. McRee, K. Moffat, E.D. Getzoff, Science 275 (1997) 1471–1475.
[3] M.P. Heyn, R.J. Cherry, J. Müller, J. Mol. Biol. 117 (1977) 607–620.
[4] S.W. Lin, R.A. Mathies, Biophys. J. 56 (1989) 653–660.
[5] N.A. Clark, K.J. Rothschild, D. Luippold, B. Simons, Biophys. J. 31 (1980) 65–96.
[6] K. Barabás, A. Dér, Z. Dancsházy, P. Ormos, L. Keszthelyi, M. Marden, Biophys. J. 43 (1983) 5–11.
[7] Y. Kimura, A. Ikegami, K. Ohno, S. Saigo, Y. Takeuchi, Photochem. Photobiol. 33 (1981) 435–439.
[8] B.A. Lewis, C. Rosenblatt, R.G. Griffin, J. Courtemanche, J. Herzfeld, Biophys. J. 47 (1985) 143–150.
[9] G.F.X. Schertler, R. Lozier, H. Michel, D. Oesterhelt, EMBO J. 10 (1991) 2353–2361.
[10] B. Borucki, H. Otto, M.P. Heyn, J. Phys. Chem. 102 (1998) 3821–3829.
[11] H. Otto, M.P. Heyn, FEBS Lett. 293 (1991) 111–114.
[12] H. Otto, C. Zscherp, B. Borucki, M.P. Heyn, J. Phys. Chem. 99 (1995) 3847–3853.
[13] B. Borucki, H. Otto, M.P. Heyn, J. Phys. Chem. 103 (1999) 6371–6383.
[14] G. Drikos, H. Rüppel, Photochem. Photobiol. 40 (1984) 93–104.
[15] Q.-Y. Shang, X. Dou, B.S. Hudson, Nature 352 (1991) 703–705.
[16] B.S. Hudson, R.R. Birge, J. Phys. Chem. A 103 (1999) 2274–2281.
[17] B. Karvaly, J.M. Fukumoto, W.D. Hopewell, M.A. El-Sayed, J. Phys. Chem. 86 (1982) 1899–1908.
[18] C. Wan, J. Qian, C.K. Johnson, Biophys. J. 65 (1993) 927–938.
[19] R.M. Esquerra, D. Che, D.B. Shapiro, J.W. Lewis, R.A. Bogomolni, J. Fukushima, D.S. Kliger, Biophys. J. 70 (1996) 962–970.
[20] M.P. Heyn, H. Otto, Photochem. Photobiol. 56 (1992) 1105–1112.
[21] Q. Song, G.S. Harms, C.K. Johnson, J. Phys. Chem. 100 (1996) 15605–15613.
[22] J.F. Nagle, S.M. Bhattacharjee, L.A. Parodi, R.H. Lozier, Photochem. Photobiol. 38 (1983) 331–339.
[23] B. Borucki, PhD thesis, Freie Universität Berlin, 1998. http://www.diss.fu-berlin.de/1998/25/indexe.htm.
[24] T.N. Earnest, P. Roepe, M.S. Braiman, J. Gillespie, K.J. Rothschild, Biochemistry 25 (1986) 7793–7798.
[25] K. Fahmy, F. Siebert, M.F. Grossjean, P. Tavan, J. Mol. Struct. 214 (1989) 257–288.
[26] K. Fahmy, F. Siebert, P. Tavan, Biophys. J. 60 (1991) 989–1001.
[27] J. Breton, E. Nabedryk, Biochim. Biophys. Acta 973 (1989) 13–18.
[28] E. Nabedryk, J. Breton, FEBS Lett. 202 (1986) 356–360.
[29] J. Seelig, Q. Rev. Biophys. 10 (1997) 353–415.
[30] V. Copié, A.E. McDermott, K. Beshah, J.C. Williams, M.

Spijker-Assink, R. Gebhard, J. Lugtenburg, J. Herzfeld, R.G. Griffin, Biochemistry 33 (1994) 3280–3286.
[31] A.S. Ulrich, M.P. Heyn, A. Watts, Biochemistry 31 (1992) 10390–10399.
[32] A.S. Ulrich, A. Watts, I. Wallat, M.P. Heyn, Biochemistry 33 (1994) 5370–5375.
[33] A.S. Ulrich, A. Watts, Solid State NMR 2 (1993) 21–36.
[34] S. Moltke, A.A. Nevzorov, N. Sakai, I. Wallat, C. Job, K. Nakanishi, M.P. Heyn, M.F. Brown, Biochemistry 37 (1998) 11821–11835.
[35] A.A. Nevzorov, S. Moltke, M.P. Heyn, M.F. Brown, J. Am. Chem. Soc. 121 (1999) 7636–7643.
[36] T. Hauss, S. Grzesiek, H. Otto, J. Westerhausen, M.P. Heyn, Biochemistry 29 (1990) 4904–4913.
[37] F. Seiff, I. Wallat, P. Ermann, M.P. Heyn, Proc. Natl. Acad. Sci. USA 82 (1985) 3227–3231.
[38] F. Seiff, J. Westerhausen, I. Wallat, M.P. Heyn, Proc. Natl. Acad. Sci. USA 83 (1986) 7746–7750.
[39] M.P. Heyn, J. Westerhausen, I. Wallat, F. Seiff, Proc. Natl. Acad. Sci. USA 85 (1988) 2146–2150.
[40] T. Hauss, G. Büldt, M.P. Heyn, N.A. Dencher, Proc. Natl. Acad. Sci. USA 91 (1994) 11854–11858.
[41] A.S. Ulrich, I. Wallat, M.P. Heyn, A. Watts, Nat. Struct. Biol. 2 (1995) 190–192.
[42] S. Moltke, I. Wallat, N. Sakai, K. Nakanishi, M.F. Brown, M.P. Heyn, Biochemistry 36 (1999) 11762–11772.
[43] C. Glaubitz, I.J. Burnett, G. Gröbner, A.J. Mason, A. Watts, J. Am. Chem. 121 (1999) 5787–5794.
[44] C. Glaubitz, A. Watts, J. Mag. Res. 130 (1998) 305–316.
[45] H. Luecke, H.-T. Richter, J.K. Lanyi, Science 280 (1998) 1934–1937.
[46] L.O. Essen, R. Siegert, W.D. Lehmann, D. Oesterhelt, Proc. Natl. Acad. Sci. USA 95 (1998) 11673–11678.
[47] H. Luecke, B. Schobert, H.-T. Richter, J.-P. Carteiller, J.K. Lanyi, J. Mol. Biol. 291 (1999) 899–911.
[48] H. Luecke, B. Schobert, H.-T. Richter, J.-P. Carteiller, J.K. Lanyi, Science 286 (1999) 255–260.
[49] H. Belrhali, P. Nollert, A. Royant, C. Menzel, J.P. Rosenbusch, E.M. Landau, E. Pebay-Peyroula, Structure 7 (1999) 909–917.
[50] K. Edman, P. Nollert, A. Royant, H. Belrhali, E. Pebay-Peyroula, J. Hajdu, R. Neutze, E.M. Landau, Nature 401 (1999) 822–826.
[51] A.U. Acuña, J. Gonzalez-Rodriguez, An. Quim. 75 (1979) 630–635.
[52] N. Grigorieff, T.A. Ceska, K.H. Downing, J.M. Baldwin, R. Henderson, J. Mol. Biol. 259 (1996) 393–421.
[53] B.D. Santarsiero, M.N.G. James, M. Mahendran, R.F. Childs, J. Am. Chem. Soc. 112 (1990) 9416–9418.
[54] Q. Song, G.S. Harms, C. Wan, C.K. Johnson, Biochemistry 33 (1994) 14026–14033.
[55] G.S. Harms, Q. Song, C.K. Johnson, Biophys. J. 70 (1996) 2352–2357.
[56] N.A. Dencher, D. Dresselhaus, G. Zaccai, G. Büldt, Proc. Natl. Acad. Sci. USA 86 (1989) 7876–7879.
[57] M.H.J. Koch, N.A. Dencher, D. Oesterhelt, H.-J. Ploehn, G. Rapp, G. Büldt, EMBO J. 10 (1991) 521–526.
[58] S. Subramaniam, M. Gerstein, D. Oesterhelt, R. Henderson, EMBO J. 12 (1993) 1–8.
[59] S. Subramaniam, M. Lindahl, P. Bullough, A.R. Faruqi, J. Tittor, D. Oesterhelt, L. Brown, J. Lanyi, R. Henderson, J. Mol. Biol. 287 (1999) 145–161.
[60] P.L. Ahl, R.A. Cone, Biophys. J. 45 (1984) 1039–1049.
[61] H. Urabe, J. Otomo, A. Ikegami, Biophys. J. 56 (1989) 1225–1228.
[62] O. Weidlich, N. Friedman, M. Sheves, F. Siebert, Biochemistry 34 (1995) 10390–10399.
[63] O. Weidlich, B. Schalt, N. Friedman, M. Sheves, J.K. Lanyi, L.S. Brown, F. Siebert, Biochemistry 35 (1996) 10807–10814.
[64] Y. Yamazaki, J. Sasaki, M. Hatanaka, H. Kandori, A. Maeda, R. Needleman, T. Shindara, K. Yoshihara, L.S. Brown, J.K. Lanyi, Biochemistry 34 (1995) 577–582.
[65] S. Hashimoto, K. Obata, H. Takeuchi, R. Needleman, J.K. Lanyi, Biochemistry 36 (1997) 11583–11590.
[66] L.O. Essen, D. Oesterhelt, Nature 392 (1998) 131–133.